

Effect of post-annealing temperature on linear and non-linear optical properties of sol-gel spin coated CdS thin films

M. Venkata Veera Prasad^{1*}, K. Thyagarajan², B. Rajesh Kumar³

¹Department of Physics, JNTU Anantapur, Anantapuramu-515 002, A.P, India

²Department of Physics, JNTUA College of Engineering, Pulivendula-516 390, A.P, India

³Department of Physics, GITAM (Deemed to be University), Visakhapatnam - 530 045, A.P, India

*Corresponding Author: mvvp.physics@gmail.com, Tel.: +91-8919702285

Available online at: www.isroset.org

Received: 22/May/2019, Accepted: 12/Jun/2019, Online: 30/Jun/2019

Abstract—Cadmium sulfide thin films were prepared by sol-gel spin coating method on glass substrates and its effect of post-annealing temperature on linear and non-linear optical properties were investigated. X-ray diffraction results showed that the grown CdS thin films exhibit cubic phase with (1 1 1) as a preferential orientation. The surface morphology of CdS thin films was characterized by using atomic force microscopy. The electrical resistivity of CdS thin films measured from the four-probe method decreased from 0.74×10^4 to $0.12 \times 10^4 \Omega \cdot \text{cm}$ with the increase of post-annealing temperature from 150 to 300°C. The optical band gap of CdS thin films is found to be 2.42 eV, whereas its band gap decreased from 2.35 to 2.21 eV with the increase of post-annealing temperature from 150 to 300°C. The normal dispersion of refractive index for CdS thin films was described using Wemple-DiDomenico single-oscillator model. The optical dispersion parameters for CdS thin films were reported in this study. The Verdet constant is calculated based on the refractive index dispersion study. The first, third order nonlinear optical susceptibility ($\chi^{(1)}$, $\chi^{(3)}$) and nonlinear refractive index $n^{(2)}$ were also determined.

Keywords— Sol-gel spin coating; CdS thin films; X-ray diffraction; Atomic force microscopy; Optical properties.

I. INTRODUCTION

Cadmium sulfide (CdS) had a wide applications in electro-optic devices such as photosensors, optical wave-guides, non-linear integrated optical devices, transducers, photoconducting cells, non-linear integrated optical devices, window layer in Cu(In,Ga)Se₂ (CIGS), CdTe heterojunction solar cells, field effect transistors, light emitting diodes, gas sensors and diluted magnetic semiconductors in spintronic devices [1-5]. CdS belongs to II-VI group semiconducting material having a direct band gap of 2.42 eV (in cubic phase) and 2.57 eV (in hexagonal phase) at room temperature. CdS exhibit in two forms namely α -CdS (hexagonal wurtzite, space group: P6₃mc) and β -CdS (cubic, zinc blende crystal structure, space group: F-43m). β -CdS forms at low temperature with a metastable phase whereas α -CdS forms at high temperatures with a stable phase; however, annealing at high temperatures can transform β -CdS to α -CdS [6].

There are different chemical and physical methods to prepare CdS thin films which include spray pyrolysis [7], metal organic chemical vapor deposition (MOCVD) [8], layer adsorption and reaction (SILAR) [9], sol-gel route [10], chemical bath deposition (CBD) [11], thermal evaporation [12], sputtering [13] and pulsed laser deposition (PLD) [14].

Among these methods, the sol-gel spin coating method is a low cost, simple and able to produce uniform films with good adherence, provides a high specific surface area, narrow pore size, better microstructural control of particles and uniform particle distribution [15,16].

Here, we report the structural, transport and optical properties of CdS thin films. Studies on the nonlinear optical properties of sol-gel spin coated CdS thin films are rare to found in the literature. The main objective of the present work is to study the effect of post-annealing temperature on linear and non-linear optical properties of CdS thin films.

II. RELATED WORK

In the present work, we reported the detailed information on optical constants, optical dispersion parameters and non-linear optical properties of CdS thin films which are of much importance for its applications in integrated optic devices such as modulators, filters, switches, etc.

III. METHODOLOGY

CdS thin films were prepared by mixing 0.6 mL of polyethylene glycol (PEG 200) with 8.9 mL of ethanol and

0.5 mL of acetic acid under stirring continuously for 90 minutes. Cadmium nitrate ($\text{Cd}(\text{NO}_3)_2 \cdot 4\text{H}_2\text{O}$) and thiourea ($\text{SC}(\text{NH}_2)_2$) (chemicals of analytical grade from Sd Fine Chem. Pvt. Ltd., Mumbai, India) were used as precursors for cadmium and sulfur source. These precursors were slowly dissolved in ethanol and stirred for 90 minutes. The as-prepared solution was slowly added to polyethylene glycol (PEG) sol with stirring for 6 hours in order to obtain the sol, which is used for preparing CdS thin films. The spin coating method was used to deposit CdS thin films on glass substrates using the above sol with a rotating spin speed of 1000 rpm for 45 seconds. The glass substrates were cleaned thoroughly with detergent laboline and then rinsed with double distilled water. Then the substrates were kept in hot chromic acid for 12 hours. After chromic acid treatment, the substrates were cleaned ultrasonically in double distilled water and acetone for 10 min. Finally, the substrates were dried under an infra-red (IR) lamp. These glass substrates were used for the preparation of CdS thin films. CdS thin films were prepared on glass substrates by sol-gel spin coating method at room temperature and post-annealed the films up to 300 °C for 1 hour.

Structural properties of CdS thin films were analyzed by glancing angle X-ray diffraction (GAXRD) using a Rigaku X-ray diffractometer with $\text{CuK}\alpha$ radiation ($\lambda=0.154$ nm) source operated at 40 kV and 40 mA. X-ray diffraction measurements were recorded in the 2θ range of 20° - 90° at a glancing angle of 2° with a scan speed of 1° min^{-1} . The surface morphology of the CdS thin films is studied by using atomic force microscope (AFM; Model: Park NX20). The thickness of the CdS films is measured by Dektak surface profilometer. The electrical measurements of CdS thin films were measured by the four-probe method and Hall effect setup. The optical transmittance spectra of the CdS thin films were recorded by using UV-Vis-NIR Spectrometer (Shimadzu MPC3600) in the wavelength range of 300-2500 nm.

IV. RESULTS AND DISCUSSION

3.1 Structural analysis

X-ray diffraction (XRD) patterns of CdS thin films prepared by sol-gel spin coating method on glass substrates at room temperature (RT) and post-annealed in the vacuum from 150 to 300°C are shown in Figure 1. The diffraction peaks observed at $2\theta = 26.46^\circ$, 44.2° , and 52.2° are indexed to (1 1 1), (2 2 0) and (3 1 1) planes of pure CdS (JCPDS Card No. 10-0454). It is noticed that all the films exhibit (1 1 1) preferred orientation with a cubic structure. Post-annealing of CdS thin films leads to improve the intensity of the diffraction peaks indicating the increase in the crystallinity of the films. The 2θ value of (1 1 1) diffraction peak shift slightly towards the higher angle and the full width at half maxima (FWHM) decreased from 0.34 to 0.17° with the

increase of annealing temperature. The decrease of FWHM leads to an increase in the crystallite size of the CdS thin films.

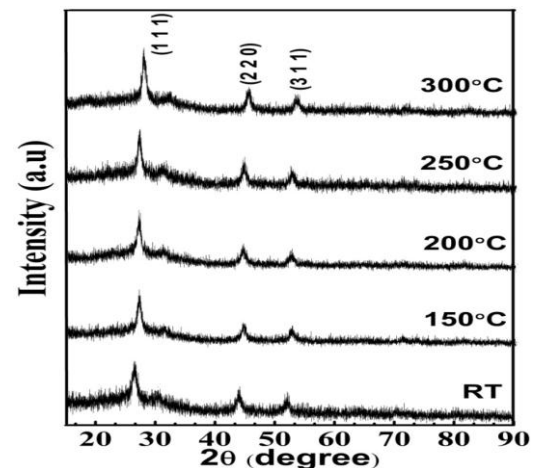


Figure 1. X-ray diffraction patterns of CdS thin films post-annealed at different temperatures.

The interplanar spacing (d) of CdS thin films is calculated using the Bragg's equation

$$2d\sin\theta = n\lambda \quad (1)$$

where θ is Bragg angle, λ is the wavelength of X-ray ($= 0.154$ nm) and n is an integer. The interplanar spacing of CdS thin films decreases from 0.3365 to 0.3342 nm with the increase of annealing temperature because of a strong interaction between the vapor atoms and the substrate and realignment of grains. The lattice constant (a) of CdS thin films was calculated from the formula

$$a = d(h^2 + k^2 + l^2)^{1/2} \quad (2)$$

for the observed d values corresponding to (h k l) plane obtained by X-ray diffraction data. The lattice constant (a) values decreases from 0.5829 to 0.5788 nm with the increase of annealing temperature due to the shift in the angular position of the prominent peak. The crystallite size (D) of CdS thin films is estimated from Scherer's formula [17]. The crystallite size value increased from 25.07 to 50.17 nm due to the decrease of grain boundary leading to higher conductivity in the films. The number of crystallites per unit area (N) is determined by using the relation

$$N = t/D^3 \quad (3)$$

where t is the thickness of the film and D is crystallite size of the films. The thickness of the films measured from surface profilometer is in the range of 190-320 nm. The thickness of CdS thin films decreased with the increase of annealing temperature from 150 to 300°C. The number of crystallites of CdS thin films decreases from 6.35×10^{15} to $1.58 \times 10^{15} \text{ m}^{-2}$ with the increase of annealing temperature from 150 to 300 °C. The structural parameters of CdS thin films post-annealed at different temperatures are given in Table 1.

Table 1. Structural parameters of CdS thin films post-annealed at different temperatures

Annealing Temp. (°C)	2θ (°)	FWHM (°)	d-spacing (nm)	Lattice constant, a (nm)	Crystallite size, D (nm)	No. of crystallites, $N \times 10^{15} (\text{m}^{-2})$
RT	26.46	0.34	0.3365	0.5829	25.07	12.68
150	26.55	0.27	0.3354	0.5809	31.58	6.35
200	26.56	0.24	0.3352	0.5806	35.53	4.46
250	26.61	0.18	0.3348	0.5798	47.38	1.88
300	26.65	0.17	0.3342	0.5788	50.17	1.58

3.2 AFM analysis

AFM images of (scan area: $2 \mu\text{m} \times 2 \mu\text{m}$) CdS thin films prepared at room temperature and post-annealed from 150 to 300 °C are shown in Figure 2.

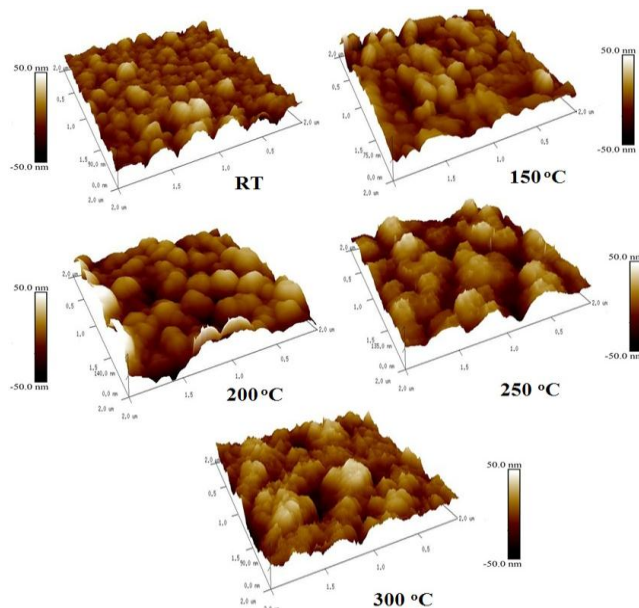


Figure 2. AFM images of CdS thin films post-annealed at different temperatures.

From AFM images, it is observed that the grain size increases with the increase of annealing temperature which is due to the increase in grain boundary movement and mobility of the thin films. The average roughness (R_a) of the CdS thin films increased from 11.4 to 17 nm, whereas the RMS roughness (R_q) values increased from 7.7 to 13 nm with the increase of annealing temperature and reach the maximum value at 300 °C. The increase in surface roughness of the films decreases the reflective loss which consequently increases the quantum efficiency of a solar cell [18]. The maximum peak height (R_p) and peak valley (R_z) values increased with increasing annealing temperature due to the enhancement in crystallinity of the films. The negative values of skewness (R_{sk}) indicate that the film had a rough surface with a low density of dips or valleys and flat regions.

When kurtosis (R_{ku}) value is equal to 3, it represents the surface with a Gaussian height distribution and the surface is called Mesokurtic, but if $R_{ku} < 3$ the surface is flat and called Platykurtic. If $R_{ku} > 3$, the surface has more number of peaks than valleys. The CdS thin films exhibit the value of $R_{ku} > 3$ and the distribution will have high number of peaks and low valleys with a spiky surface on the films. The statistical analysis of CdS thin films obtained from AFM is given in Table 2.

Table 2. Surface roughness parameters of CdS thin films.

Annealing temp. (°C)	R_a (nm)	R_q (nm)	R_z (nm)	R_p (nm)	R_v (nm)	R_{sk}	R_{ku}
RT	11.4	7.7	4.4	30.1	-31.8	-0.55	4.17
150	13.5	8.5	8.3	33.6	-38.4	-0.30	3.98
200	10.2	9.3	17.2	34.1	-26.4	-1.06	5.19
250	16.2	12.8	20.6	36.7	-39.6	-0.17	5.18
300	17	13	22.1	45.3	-43.6	-0.40	4.10

3.3 Electrical properties

The electrical resistivity (ρ) of the CdS thin films were measured by using a four-probe method. The electrical resistivity of CdS thin film at room temperature is found to be $1.47 \times 10^5 \Omega \cdot \text{cm}$, whereas its resistivity decreased from 0.74×10^4 to $0.12 \times 10^4 \Omega \cdot \text{cm}$ with the increase of annealing temperature from 150 to 300 °C. The electrical resistivity of the films is decreased due to the decrease in density grain boundary intercrystallites and defects such as pinholes, voids, etc. The obtained electrical resistivity values are in good agreement with previously reported works [19,20]. The carrier concentration (n_c) and mobility (μ_H) of the CdS thin films is measured from Hall effect apparatus at room temperature in a magnetic field of 0.35T [21]. The sign of Hall voltage across the samples is negative, indicating n-type semiconducting behavior of the films. The carrier concentration of CdS thin films increased from 0.76×10^{13} to $1.96 \times 10^{13} \text{ cm}^{-3}$ with the increase of annealing temperature from 150 to 300 °C. The increase in the carrier concentration of the films causes shrinkage in the gap known as the bandgap narrowing, which signifies that the density of dislocations and density of grain boundaries will be decreased [22]. The carrier concentration is in the order of 10^{13} cm^{-3} for all the films and these values are in good agreement with chemical bath deposited CdS thin films [23,24]. The Hall mobility of the films increased from 110 to $258 \text{ cm}^2 \text{ V}^{-1} \text{ s}^{-1}$ with the increase of annealing temperature from 150 to 300 °C due to the increase in the grain size and reducing grain boundary scattering. The mean free path (L) of an electron can be calculated using the equation [25]

$$L = (3\pi^2)^{1/3} (h/2\pi e^2) \cdot 1/\rho \cdot n_c^{2/3} \tag{4}$$

here h is Planck's constant, e is the electron charge, ρ is the resistivity, and n_c is the carrier concentration. The mean free path (L) of an electron of CdS thin films is found to be increased with the increase of annealing temperature. The longest mean free path of 4.73 nm is obtained for the film annealed at 300 °C. These values of mean free path are much shorter than the grain size measured according to XRD analysis. The effect of scattering at grain boundaries and dislocations may be neglected because the mean free path is smaller than the grain size, and scattering of conduction electrons mainly depend on ionized and neutral impurities. The electrical properties of CdS thin films post-annealed at different temperatures are given in Table 3.

Table 3. Electrical properties of CdS thin films post-annealed at different temperatures

Ann. Temp. (°C)	Type	Electrical resistivity, ρ ($\Omega \cdot \text{cm}$)	Carrier concentration, $n_c \times 10^{13}$ (cm^{-3})	Hall-mobility, μ_H ($\text{cm}^2 \text{V}^{-1} \text{S}^{-1}$)	Mean free path, L (nm)
RT	n	1.47×10^5	0.68	62	3.34
150	n	0.74×10^4	0.76	110	3.46
200	n	0.47×10^4	0.86	154	3.61
250	n	0.26×10^4	1.01	231	3.80
300	n	0.12×10^4	1.96	258	4.73

3.4 Optical properties

3.4.1 Optical transmittance and energy band gap

The optical transmittance spectra of the CdS thin films post-annealed at different temperatures are shown in Figure 3(a). The shift in absorption edge towards longer wavelengths with an increase in post-annealing temperature indicates the growth of the particles. The average optical transmittance of CdS thin films (in the UV-Vis region) increased from 65 to 82% with the increase of annealing temperature which may be caused by lattice imperfections, reduction in voids, film thickness and increase in the crystallite size. The optical constants of CdS thin films were calculated from the equations as reported in the earlier literature [26]. The absorption coefficient (α) values of CdS thin films at the wavelength 550 nm increases from 1.30×10^4 to $2.03 \times 10^4 \text{ cm}^{-1}$ with the increase of annealing temperature from 150 to 300 °C. The extinction coefficient (k) values (at $\lambda=550 \text{ nm}$) increases from 0.062 to 0.097 with the increase of annealing temperature from 150 to 300 °C. The optical band gap of the CdS thin films was determined by using the Tauc's formula [27,28]. Figure 3(b) shows the extrapolation of $(\alpha h\nu)^2$ versus $h\nu$ with the intercept of the straight line on $h\nu$ axis.

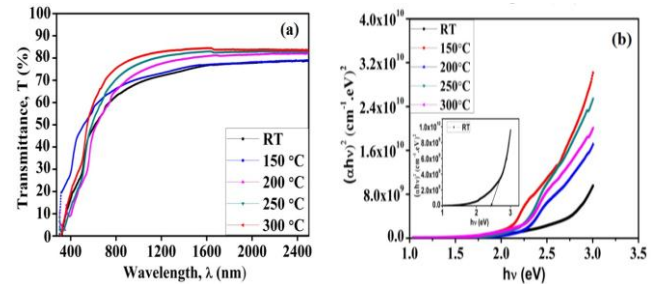


Figure 3. (a) Optical transmittance spectra and (b) Tauc's plot for CdS thin films.

The optical band gap of CdS thin films at room temperature is found to be 2.42 eV. The optical band gap values of the films decreased from 2.35 to 2.21 eV with the increase of post-annealing temperature from 150 to 300 °C because of increase in the particle size and quantum size effect. During annealing, the recrystallization process densified the film and eliminates the defects present in the material [29]. The obtained direct band gap values for cubic CdS thin films are in good agreement with the previously reported values [30,31]. The refractive index (n) of CdS thin films annealed at different temperatures was calculated using the equations as reported in the earlier literature [32]. The variation of refractive index with wavelength for CdS thin films post-annealed at different temperature are shown in Figure 4(a). The refractive index (n) of the films decreased from 2.30 to 1.90 with the increase of annealing temperature from 150 to 300 °C due to the improvement in crystallinity of the films. H. Metin et al [33] reported similar behavior in the change of the refractive index for the CdS thin films prepared by the chemical deposition method.

3.4.2 Optical dispersion, group and phase velocity

The optical dispersion study is an important parameter to understand the optical properties of the films. Figures 4(b)-(d) shows the optical dispersion, group and phase velocity of films with photon wavelength respectively. It is observed that optical dispersion $dn/d\lambda$ of the film depends on both annealing temperature and wavelength. The group velocity, U_g which describes pulse propagation through an isotropic medium with undistorted shape is given by the following relation [34]

$$U_g = d\omega/dk = c / [n - \lambda (dn/d\lambda)] \quad (5)$$

where c is the velocity of light in vacuum, k is the wave number, ω is the angular frequency of the incident light. The wavelength dependence of the group velocity and phase velocity for the CdS thin film is shown in Figure 4(b).

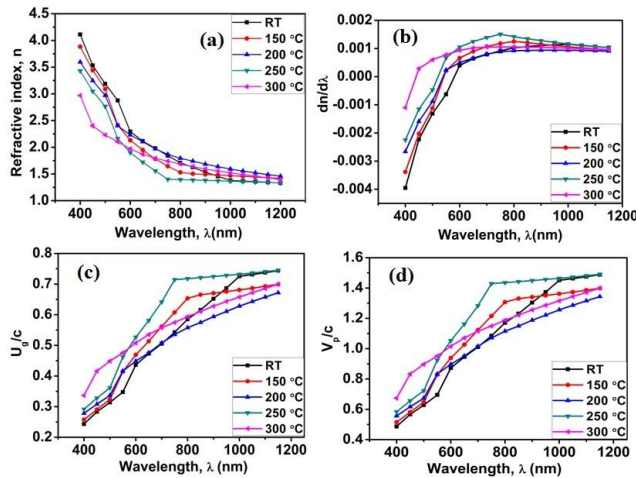


Figure 4. Variation of (a) refractive index, n ; (b) optical dispersion, $dn/d\lambda$; (c) group velocity, U_g/c and (d) Phase velocity, v_p/c of CdS thin films as a function of wavelength.

The results show that the group velocity and phase velocity for CdS thin films increases with wavelength and decreases with annealing temperature which is due to the optical dispersion in the material.

3.4.3 Magneto-optical constant: Verdet coefficient V

The Verdet coefficient (V) is defined as the single pass volume Faraday rotation per unit magnetic field and unit thickness. The Verdet coefficient is measured using two Glan-Taylor polarizers, but in the present study, we estimated V from the refractive index dispersion data [35]. The refractive index (n) is related to V with the following equation

$$V(\lambda) = \mu_0 r \cdot (e/2mc) \lambda \, dn/d\lambda \quad (6)$$

where μ_0 is the vacuum permeability, r is the magneto-optical anomaly factor whose value is close to 0.28 for materials exhibiting covalent bond character and 1 for materials showing ionic type bond, e is the charge of electron, m is the mass of electron, c is the velocity of light and $dn/d\lambda$ is the optical dispersion of the material. The wavelength dependence of the Verdet coefficient is shown in Figure 5, we noticed that the Verdet coefficient takes negative and positive values and mainly dependent on the band gap in the negative part.

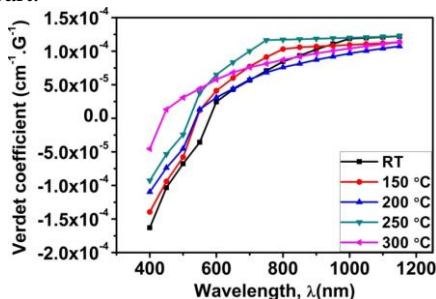


Figure 5. Variation of Verdet coefficient dispersion of CdS thin films.

3.5 Optical dispersion parameters

The refractive index dispersion data for CdS thin films is analyzed in terms of the single effective oscillator model proposed by Wemple-DiDomenico (WDD) [36]. The energy parameters single-oscillator energy (E_o) and dispersion energy (E_d) is introduced and the refractive index (n) at any photon energy $h\nu$ is expressed by the Wemple-DiDomenico relationship [37]

$$n^2 - 1 = 1 - E_o E_d / (E_o^2 - E^2) \quad (7)$$

The dispersion parameters E_o and E_d are obtained from the slope $(E_o E_d)^{-1}$ and the intercept E_o/E_d on the vertical axis of the straight line portion of the $(n^2 - 1)^{-1}$ against $(h\nu)^2$ plot as shown in Figure 6(a). The values of E_o and E_d obtained from the linear fitting are reported in Table 4. The values of E_o and E_d decreases with increasing post-annealing temperature, which confirms the decrease in the optical band gap of the films with increasing annealing temperature. The single-oscillator parameters of the oscillator energy E_o , and the dispersion energy E_d are given by

$$E_o^2 = M_{-1}/M_{-3} \quad (8)$$

$$E_d^2 = M_{-1}^3/M_{-3} \quad (9)$$

where M_{-1} and M_{-3} are the -1 and -3 moments of the optical spectrum, respectively [38,39]. The calculated values of M_{-1} and M_{-3} are given in Table 4. M_{-1} values decreased from 1.31 to 0.77 and M_{-3} values decreased from 0.23 to 0.18 (eV)².

The average interband oscillator wavelength (λ_o) and average oscillator strength (S_o) for CdS thin films can be determined by using the single Sellmeier oscillator relation [40]

$$n^2 - 1 = S_o \lambda_o^2 / (1 - (\lambda_o/\lambda)^2) \quad (10)$$

where S_o is the average oscillator strength, and λ_o is the average oscillator wavelength. The S_o and λ_o are obtained from the slope and the intercept on the vertical axis of the straight-line portion of the $(n^2 - 1)^{-1}$ versus λ^2 plot shown in Figure 6(b). The intersection with $(n^2 - 1)^{-1}$ axis is $(n_\infty^2 - 1)^{-1}$ and hence, n_∞^2 at λ_o equal to high frequency dielectric constant (ϵ_∞).

The dielectric constant is partially due to free electrons and bound electrons as represented with the following relation [41]

$$\epsilon_1 = n^2 = \epsilon_L - (e^2 N / 4\pi \epsilon_o c^2 m^*) \lambda^2 \quad (11)$$

where ϵ_L is the lattice dielectric constant and N/m^* is the ratio of carrier concentration to its effective mass. The dependence of n^2 with λ^2 for CdS thin films is shown in Figure 6(c) which exhibits linear, ϵ_L and N/m^* values are estimated from the intercept and slope of the plot. It is found that the values of ϵ_L and N/m^* are increased with increasing annealing temperature, which is due to the increase in free charge carrier density and low lattice phonon interaction. The values of ϵ_∞ , ϵ_L , and N/m^* are given in Table 4.

The characteristic frequency at which the material changes from metallic to dielectric response is known as plasma

frequency (ω_p). According to the Drude free-electron model, the plasma frequency ω_p is given as

$$\omega_p^2 = e^2 N/m^* \epsilon_0 \tag{12}$$

The plasma resonance frequency (ω_p) of all valence electrons involved in the optical transitions was calculated using the above relation and the values for CdS thin films are reported in Table 4. The increase in free carrier concentration of CdS thin films upon annealing favours the increase in plasma frequency of CdS thin films.

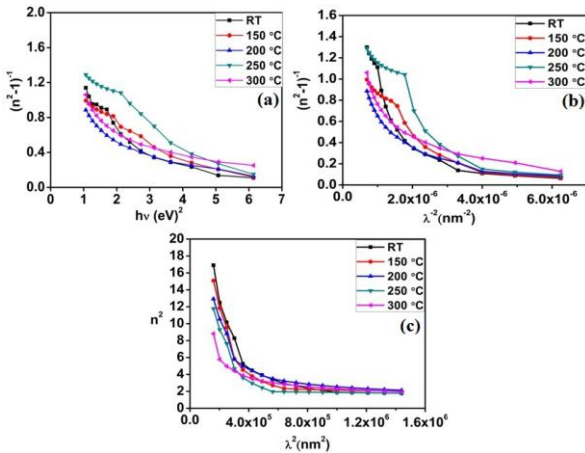


Figure 6. Plots of (a) $(n^2-1)^{-1}$ Vs $(hv)^2$, (b) $(n^2-1)^{-1}$ Vs λ^2 , and (c) n^2 Vs λ^2 for CdS thin films

3.6 Nonlinear optical properties

Nonlinear optics study plays a key role in understanding fundamental applications of all optical circuits, optical signals processing units, and switching devices. In nonlinear media the dielectric polarization, P shows nonlinear behaviour with the electric field, E of the incident light. Thus the non-linear electron polarizability P_{NL} can be shown by the equation as given below [42,43]

$$P = \chi^{(1)} E + P_{NL} \tag{13}$$

where $P_{NL} = \chi^{(2)} E^2 + \chi^{(3)} E^3$, where $\chi^{(1)}$ is linear optical susceptibility, $\chi^{(2)}$ and $\chi^{(3)}$ are second and third order non-linear optical susceptibilities. The linear optical susceptibility, $\chi^{(1)}$ of a medium can be written by the following equation [44]

$$\chi^{(1)} = (n^2-1)/4\pi \tag{14}$$

$\chi^{(3)}$ is a parameter which indicates that the films are appropriate for optical switching and photonic applications. According to Miller's generalized rule, the relation between third-order nonlinear optical susceptibility, $\chi^{(3)}$ and linear optical susceptibility, $\chi^{(1)}$ is given as

$$\chi^{(3)} = A (\chi^{(1)})^4 \tag{15}$$

From Eq. (14) and Eq. (15), we can obtain the following relation

$$\chi^{(3)} = A(n^2-1)^4/(4\pi)^4 \tag{16}$$

where $A \approx 1.7 \times 10^{-10}$ esu, is a quantity that is independent of frequency and mostly it is the same for all materials [45,46]. The nonlinear refractive index $n^{(2)}$ is an important parameter

for manufacturing efficient and reliable optoelectronic devices. The nonlinear refractive index $n^{(2)}$ is directly related to third-order nonlinear optical susceptibility, $\chi^{(3)}$. Tichy and Ticha relation gives a combination of the Miller's generalized rule and n_0 obtained from WDD model which is given by the equation

$$n^{(2)} = 12 \pi \chi^{(3)} / n_0 \tag{17}$$

Figures 7(a-c) shows the results of linear optical susceptibility $\chi^{(1)}$, third order non-linear optical susceptibility $\chi^{(3)}$ and nonlinear refractive index $n^{(2)}$ as a function of photon energy ($h\nu$) for CdS thin films.

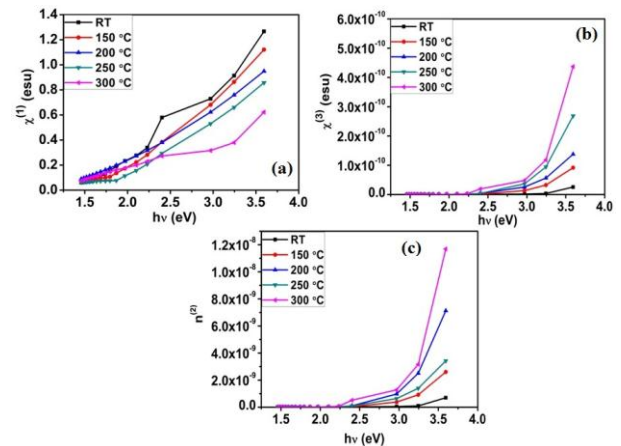


Figure 7. Variation of (a) first order linear susceptibility, $\chi^{(1)}$; (b) third order nonlinear susceptibility, $\chi^{(3)}$; and (c) nonlinear refractive index, $n^{(2)}$ with energy for CdS thin films.

The behavior of the nonlinear refractive index is same as a third order nonlinear optical susceptibility as a function of energy. It can be observed that the annealing temperature improves the non-linear response. In the present work, the third order nonlinear optical susceptibility value was observed to be high as compared to the earlier reported values for CdS thin films [47,48]. The results show that this CdS thin films exhibit large third-order nonlinear optical susceptibility which makes it potentially useful for nonlinear optical devices.

Table 4. Optical dispersion parameters of CdS thin films

Parameter	RT	150 °C	200 °C	250 °C	300 °C
E_g (eV)	2.42	2.35	2.28	2.25	2.21
E_o (eV)	2.96	2.39	2.17	1.78	1.77
E_d (eV)	3.14	2.69	2.15	1.83	1.36
M_1	1.31	1.03	0.99	0.91	0.77
M_3 (eV ⁻²)	0.32	0.24	0.23	0.21	0.18
λ_o (nm)	418	520	570	696	700
S_o (10 ¹² m ⁻²)	6.06	4.18	3.04	2.12	1.57

ϵ_{∞}	1.77	1.91	1.99	2.03	2.31
ϵ_L	3.72	4.51	4.89	5.66	5.95
$N/m^*(10^{49} \text{ cm}^{-3} \text{ g}^{-1})$	2.98	3.31	3.59	3.67	5.10
$\omega_p (10^{13} \text{ Hz})$	3.59	4.34	4.73	5.39	5.64

V. CONCLUSION AND FUTURE SCOPE

CdS thin films were successfully synthesized by sol-gel spin coating method and post-annealing in the vacuum from 150 to 300 °C for 1 hour. X-ray diffraction studies of CdS thin films show cubic structure with preferential growth along the (111) plane. The surface morphology of the CdS thin films shows that the grain size increased with the increase of annealing temperature from 150 to 300 °C. The optical transmittance and band gap of CdS thin films decreased from 2.42 to 2.21eV with the increase of annealing temperature from 150 to 300 ° due to the quantum confinement effect. The Verdet coefficient for the CdS thin films was calculated from the dispersion of the refractive index. It exhibits a spread negative range which was dependent on the optical band gap energy. The dispersion of the refractive index of CdS thin films was analyzed by applying the Wemple-DiDomenico single oscillator model. The optical dispersion parameters such as the oscillator resonance energy E_o and oscillator dispersion energy E_d decreased with increasing annealing temperature. The nonlinear optical parameters linear optical susceptibility $\chi^{(1)}$, nonlinear optical susceptibility $\chi^{(3)}$, and nonlinear refractive index $n^{(2)}$ are also reported. The future scope of CdS thin films was found to be appropriate for designing nonlinear optical devices/optoelectronic devices.

ACKNOWLEDGMENT

The authors would like to convey a special gratitude to CeNSE (Center of Nano Science and Engineering), Indian Institute of Science (IISc), Bangalore, India for providing the necessary facilities for this research work under INUP (Indian Nanoelectronics Users Program).

REFERENCES

- [1] Han Jun-feng, Fu Gan-hua, V. Krishnakumar, Liao Cheng, Wolfram Jaegermann, "CdS annealing treatments in various atmospheres and effects on performances of CdTe/CdS solar cells", J. Mater. Sci.: Mater. Electron., Vol.24, No.8, pp.2695-2700, 2013.
- [2] S.H.Mousavi, M.H. Jilavi, T.S. Muller, P.W. de Oliveira, "Formation and properties of cadmium sulfide buffer layer for CIGS solar cells grown using hot plate bath deposition", J. Mater. Sci.: Mater. Electron., Vol.25, No.6, pp.2786-2794, 2014.
- [3] M. Esmaili-Zare, M. Behpour, "Fabrication and study of optical properties on CdS semiconductor as buffer layer for Cu(In, Ga)Se₂ thin film solar cells", J. Mater. Sci.: Mater. Electron., Vol.28, No.14, pp.10173-10183, 2017.
- [4] G.Ojeda-Barrero, A.I. Oliva-Aviles, A.I.Oliva, R.D.Maldonado, M. Acosta, G.M. Alonzo-Medina, "Effect of the substrate temperature on the physical properties of sprayed-CdS films by using an automatized perfume atomizer", Mater. Sci. Semicond Process. Vol.79, pp.7-13, 2018.
- [5] P.K. Mochahari, "Investigation of Structural and Spectroscopic Properties of Nanostructured CdS Films", International Journal of Scientific Research in Physics and Applied Sciences, Vol.5, Issue.6, pp.1-4, 2017. [6] Shadia J. Ikhmayies, "Characterization of nanomaterials", JOM., Vol. 66, No.,1, pp.46-60, 2014.
- [7] A.A. Yadav, E.U. Masumdar, "Photoelectrochemical investigations of cadmium sulphide (CdS) thin film electrodes prepared by spray pyrolysis", J. Alloys Compd., Vol.509, No.17, pp.5394-5399, 2011.
- [8] M. Tsuji, T. Aramoto, H. Ohyama, T. Hibino, K. Omura, "Characterization of CdS thin film in high efficient CdS/CdTe solar cells", J. Cryst. Growth., Vol. 214, pp.1142-1147, 2000.
- [9] S.D. Sartale, C.D.Lokhande, "Growth of copper sulphide thin films by successive ionic layer adsorption and reaction (SILAR) method", Mater. Chem. Phys., Vol.65, No.1, pp.63-67, 2000.
- [10] A.A. Ziabari, F.E. Ghodsi, "Growth, characterization and studying of sol-gel derived CdS nanocrystalline thin films incorporated in polyethyleneglycol: Effects of post-heat treatment", Sol. Energy Mater. Sol. Cells., Vol.105, pp.249-262, 2012.
- [11] M.A. Mahdi, Z. Hassan, S.S. Ng, J.J. Hassan, S.K. Mohd Bakhori, "Structural and optical properties of nanocrystalline CdS thin films prepared using microwave-assisted chemical bath deposition", Thin Solid Films, Vol.520, No.9, pp.3477-3484, 2012.
- [12] Salah Abdul-Jabbar Jassim, Abubaker A. Rashid Ali Zumaila, Gassan Abdella Ali Al Waly, "Influence of substrate temperature on the structural, optical and electrical properties of CdS thin films deposited by thermal evaporation", Results Phys., Vol. 3, pp.173-178, 2013.
- [13] Nam-Hoon Kim, Seung-Han Ryu, S.Hyo-Sup Noh, Woo-Sun Lee, "Electrical and optical properties of sputter-deposited cadmium sulfide thin films optimized by annealing temperature", Mater. Sci. Semicond Process., Vol. 15, No.2, pp.125-130, 2012.
- [14] P. Kumar, N. Saxena, R. Chandra, K. Gao, S. Zhou, A. Agarwal, F. Singh, V. Gupta, D. Kanjilal, "SHI induced enhancement in green emission from nanocrystalline CdS thin films for photonic applications", J. Lumin., Vol. 147, pp.184-189, 2014.
- [15] D.M.C.U. Dissanayake, P. Samarasekara, "Optical and Structural Properties of Spin Coated Cadmium Sulfide Thin Films", J. Sci. Univ. Kelaniya, Vol. 10, pp.13-20, 2015.
- [16] M.A. Aegerter, R. Almeida, A. Soutar, K. Tadanaga, H. Yang, T. Watanabe, "Coatings made by sol-gel and chemical nanotechnology", J. Sol. Gel. Sci. Tech., Vol. 47, No.2, pp.203-236, 2008.
- [17] B.D. Cullity, "Elements of X-ray diffraction", Addison-Wiley Reading, M.A., USA, pp.1-514, 1972.
- [18] E. Akbarnejab, Z. Ghorannevis, F. Abbasi, M. Ghorannevis, "Investigation of annealing temperature effect on magnetron sputtered cadmium sulfide thin film properties", J. Theor. Appl. Phys., Vol.11, No.1, pp.45-49, 2017.
- [19] A. Kriper, E. Guneri, F. Gode, C. Gumus, T. Ozposan, "The structural, electrical and optical properties of CdS thin films as a function of pH", Mater. Chem. Phys., Vol. 129, pp.183-188, 2011.
- [20] J. Santos Cruz, R.C. Perez, G.T. Delgado, O.Z. Angel, "CdS thin films doped with metal-organic salts using chemical bath deposition", Thin Solid Films, Vol. 518, No.7, pp. 1791-1795, 2010.
- [21] B. Hymavathi, B. Rajesh Kumar, T. Subba Rao, "Post-Annealing Effects on Surface Morphological, Electrical and Optical

- Properties of Nanostructured Cr-Doped CdO Thin Films*", J. Electron. Mater. Vol. **47**, No.1, pp.503-511, 2018.
- [22] M. Özta, M. Bedir, M.Y. Hacıibrahmoglu, Y. Özdemir, S. Mert, "Comparison of the Structural Electrical and Optical Properties of CdS Films Deposited by Chemical Bath Deposition and Spray Pyrolysis", Nanomed. Nanotechnol. Vol.3, No.1, pp.000130(1-8), 2018.
- [23] Deokjoon Cha, Sunmi Kim, N.K. Huang, "Study on electrical properties of CdS films prepared by chemical pyrolysis deposition", Mater. Sci. Eng. B: Solid State Mater. Adv. Technol., Vol. **106**, pp.63-68, 2004.
- [24] Fangyang Liu, Yanqing Lai, Jun Liu, Bo Wang, Sanshuang Kuang, Zhian Zhang, Jie Li, Yexiang Liu, "Characterization of chemical bath deposited CdS thin films at different deposition temperature", J. Alloy. Compd., Vol.493, No.1, pp.305-308, 2010.
- [25] Nasreddine Beji, Mehdi souli, Meriem Reghima, Sonia Azzaza, Alleg Safia, Najoua Kamoun-Turki, "Effects of Molybdenum Doping and Annealing on the Physical Properties of In₂O₃ Thin Films", J. Electron. Mater., Vol.46, No.11, pp.6628-6638, 2017.
- [26] B. Hymavathi, B. Rajesh Kumar, T. Subba Rao, "Influence of sputtering power on structural, electrical and optical properties of reactive magnetron sputtered Cr doped CdO thin films", J. Mater. Sci: Mater. Electron., Vol. **28**, No.10, pp.7509-7516, 2017.
- [27] J. Tauc (ed.), Amorphous and Liquid Semiconductors (Plenum Press, New York, 1974).
- [28] B. Srinivasa Rao, V. Rajagopal Reddy, B. Rajesh Kumar, T. Subba Rao, "Synthesis and characterization of nickel doped CdS nanoparticles", Int. J. Nano Sci., Vol.11, pp.124006(1-5), 2012.
- [29] Soumya R. Deo, Ajaya K. Singh, Lata Deshmukh, L. J. Paliwal, R.S. Singh, Rameshwar Adhikari, "Structural, morphological and optical studies on chemically deposited nanocrystalline CdZnSe thin films", J. Saudi Chem. Soc., Vol. **18**, No.4, pp.327-339, 2014.
- [30] A. A. Yadav, M. A. Barote, E.U. Masundar, "Studies on nanocrystalline cadmium sulphide (CdS) thin films deposited by spray pyrolysis", Solid State Sci., Vol.12, No.7, pp.1173-1177, 2010.
- [31] Qiu Jijun, Jin Zhengguo, Wu. Weiging, Liu Xiaoxin, Cheng Zhijie, "Effect of annealing on structural, optical and electrical properties of CdS thin films grown by ILGAR", J. Wuhan Univ. Technol. Mater. Sci. Ed., Vol. **21**, pp.88-91, 2006.
- [32] B. Rajesh Kumar, T. Subba Rao, "Investigations on optoelectronic properties of DC reactive magnetron sputtered zinc aluminum oxide thin films annealed at different temperatures", Appl. Surf. Sci., Vol.265, pp.169-175, 2013.
- [33] H. Metin, R. Esen, "Annealing studies on CBD grown CdS thin films", J. Cryst. Growth, Vol. **258**, pp.141-148, 2003.
- [34] D. Abdelkader, F. Chaffar Akkari, N. Khemiri, R. Miloua, F. Antoni, B. Gallas, M. Kanzari, "Effect of SnS addition on the morphological and optical properties of (SnS)_m(Sb₂S₃)_n nanorods elaborated by glancing angle deposition", Phys. B: Condens. Matter., Vol. **546**, pp.33-43, 2018.
- [35] R. Hamrouni, N. E. H. Segmane, D. Abdelkade, A. Amara, A. Drici, M. Bououdina, F. Chaffar Akkari, N. Khemiri, L. Bechiri, M. Kanzari, J. C. Bernède, "Linear and non-linear optical properties of Sb₂Se₃ thin films elaborated from nano-crystalline mechanically alloyed powder", Appl. Phys. A, Vol.124, pp.861(1-10), 2018.
- [36] S.H. Wemple, M. DiDomenico, "Behavior of the Electronic dielectric constant in covalent and ionic materials", Materials, Phys. Rev. B, Vol. **3**, pp.1338-1351, 1971.
- [37] S.H. Wemple, M. DiDomenico, "Refractive-Index Behavior of Amorphous Semiconductors and Glasses", Phys. Rev. B, Vol. **7**, No.8, pp.3767-3777, 1973.
- [38] S.H. Wemple, M. DiDomenico, "Optical dispersion and the structure of solids", Phys. Rev. Lett., Vol. **23**, pp.1156-1160, 1969.
- [39] A.M. Salem, "Structure, refractive-index dispersion and the optical absorption edge of chemically deposited Zn_xCd_(1-x)S thin films", Appl. Phys. A, Vol. **74**, No.2, pp.205-211, 2002.
- [40] M. DiDomenico, S.H. Wemple, "Oxygen-Octahedra Ferroelectrics. I. Theory of Electro-optical and Nonlinear optical Effects", J. Appl. Phys., Vol. **40**, No.2, pp.720-734, 1969.
- [41] Edward D. Palik, *Handbook of Optical Constants of Solids* (Academic Press Handbook, New York, 1985).

AUTHORS PROFILE

Mr.M.Venkata Veera Prasad, pursuing Ph.D in JNTU Anantapur, Anantapuramu, under the guidance of Dr. K. Thyagarajan, Professor & Head, Department of Physics, JNTUA College of Engineering, Pulivendula, Andhra Pradesh, India. He is presently working as Assistant Professor in Physics, Vaagdevi Institute of Technology & Science, Proddatur, Andhra Pradesh. His main research work is on Thin films by Sol-gel Spin Coating method.



Dr. K. Thyagarajan, Professor & Head, Department of Physics, JNTUA College of Engineering, Pulivendula, Andhra Pradesh, India. He obtained his Ph.D degree in Physics with specialization Spectroscopy from Sri Venkateswara University, Tirupati, A.P. He has more than 55 research publications to his credit, published in reputed national and international journals and attended many national and international conferences. He has presented more than 50 papers in seminars, national and International conferences. He has guided so far nine Ph.D students and at present eight students are pursuing Ph.D under his guidance.



Dr. B. Rajesh Kumar is an Assistant Professor in Physics, GIT, GITAM University, Visakhapatnam, A.P. He obtained his Ph.D degree in Physics with specialization Materials Science-Thin Film Physics from Sri Venkateswara University, Tirupati, A.P. He has published more than 25 research papers in reputed international journals and attended many national and international conferences. He is a life member of the Materials Research Society of India (MRSI), Indian Vacuum Society (IVS) and Electron Microscope Society of India (EMSI).

